Characterization of Magnetized Microplasmas for Etching Processes in Next-Generation Bipolar Semiconductor Device Fabrication

Munir M. Nafeh

Faculty of Engineering Physics, Accra Technical University, Accra, GHANA
Email: munirnafeh@gmail.com

Abstract
A compact, low-pressure magnetized microplasma source was developed to enhance etching precision in advanced semiconductor fabrication. Diagnostics using Langmuir probes and optical emission spectroscopy revealed highly anisotropic ion energy distributions influenced by external magnetic fields. The plasma exhibited superior uniformity and controllable electron density gradients. Simulation results indicate that optimized magnetic confinement improves surface smoothness and minimizes substrate damage. This study establishes a foundation for scalable, energy-efficient plasma tools in nanoscale patterning and microelectronics manufacturing. This research addresses the critical need for advanced plasma sources capable of achieving the stringent uniformity, selectivity, and anisotropy requirements of next-generation semiconductor etching processes, particularly as feature sizes approach the sub-10 nm scale.

Keywords: Magnetized plasmas; Microplasmas; Next-generation; Semiconductor etching
Received: October 2025; **Revised:** December 2025; **Accepted:** December 2025; **Published:** January 2026

1. Introduction

Traditional capacitively coupled plasma (CCP) and inductively coupled plasma (ICP) reactors, while foundational to modern microfabrication, are increasingly challenged by issues such as aspect ratio dependent etching (ARDE), plasma non-uniformity across large-diameter wafers, and the generation of damaging high-energy ions and electrons. These limitations stem fundamentally from the inherent characteristics of these sources, including electron heating mechanisms, sheath dynamics, and the spatial distribution of the plasma [1-4]. To overcome these barriers, a paradigm shift in plasma source design is necessary, moving toward systems that allow for finer, external control over key plasma parameters namely, electron temperature (T_e) and ion energy distribution (IED) [5-7]. The concept of magnetized microplasmas represents a promising avenue for this advancement [8-10].

Microplasmas, defined by their characteristic dimensions often in the sub-millimeter range, naturally operate at elevated pressures and high-power densities, leading to high radical and ion densities with a relatively low electron temperature, which is beneficial for reducing etch damage and enhancing selectivity [11-13]. Furthermore, the inherent small scale offers the potential for high spatial resolution and modularity, allowing for a more uniform and scalable distribution of plasma sources across increasingly large wafers (e.g., 450 mm) [14]. The introduction of an external magnetic field significantly enhances the control capabilities of these microplasmas [15]. By applying a magnetic field, the electron gyroradius is reduced, effectively confining electrons and altering their transport and heating mechanisms. This magnetic confinement facilitates the maintenance of a high plasma density even at lower gas pressures, and, crucially, it allows for the decoupling of plasma density from electron temperature; a control knob largely absent in conventional plasma sources [16-19]. The magnetic field can be tailored to shape the electron energy distribution function (EEDF), promoting the creation of specific reactive species necessary for highly selective etching chemistries [20]. Moreover, the directed transport and reduced diffusion of magnetized electrons can significantly influence the sheath potential and ion trajectories near the wafer surface, offering an unprecedented level of control over the mean ion energy and the angular distribution of ion flux incident on the substrate, thereby minimizing critical dimension (CD) variations and reducing sidewall damage [21-25].

This work systematically investigate the influence of key operational parameters such as gas pressure, input power, and magnetic field strength and configuration; on critical plasma characteristics, including electron temperature, plasma density, and

the composition of reactive species as measured by Langmuir probe diagnostics and optical emission spectroscopy (OES).

2. Experimental Part

The experimental investigation was conducted to characterize the physical and electrical properties of magnetized microplasmas relevant to advanced semiconductor etching applications. Figure (1) shows schematically the principle of semiconductor processing with microplasma. The experimental setup consisted of a custom-designed microplasma reactor operating at sub-Torr pressures, with integrated magnetic field control and diagnostic access ports. The plasma source was a capacitively coupled configuration using a pair of parallel electrodes separated by 500 µm. The powered electrode, made of aluminum with a diameter of 10 mm, was connected to a 13.56 MHz RF power supply through a matching network, while the grounded electrode was embedded in a quartz substrate holder. The working gas, primarily argon with controlled admixtures of CF_4 and O_2, was introduced into the chamber through a precision mass flow controller system, ensuring total flow rates between 5 and 20 sccm. The base pressure was maintained at 10^{-6} Torr using a turbomolecular pump, and operational pressures were stabilized between 0.1 and 1 Torr using a throttle valve.

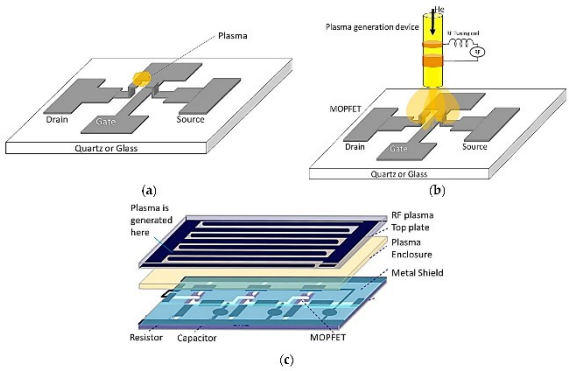

Fig. (1) Schematic explanation of semiconductor processing with microplasmas [26]

A set of neodymium permanent magnets was positioned around the discharge region to generate a uniform magnetic field of 0–200 Gauss perpendicular to the electrode plane. The field strength and uniformity were verified using a three-axis Hall probe. This magnetized configuration was employed to enhance plasma confinement, electron density, and anisotropy, all of which are critical for directional etching. The reactor geometry and magnetic field topology were optimized to simulate the microreactor conditions expected in high-aspect-ratio semiconductor structures [27].

Optical emission spectroscopy (OES) was employed to monitor excited species and determine relative concentrations of reactive radicals, including CF, F, and O, across different magnetic field configurations. The emission spectra were collected through a quartz window using a fiber-coupled spectrometer with a 0.1 nm resolution.

Langmuir probe measurements were conducted using a cylindrical tungsten probe (100 µm diameter, 2 mm length) inserted into the plasma edge to obtain electron temperature and plasma density profiles. The probe signals were analyzed using standard I–V characterization techniques with correction for RF fluctuations. Additionally, a retarding field energy analyzer (RFEA) was positioned downstream of the plasma to measure ion energy distributions relevant to etch rate control.

All measurements were conducted under steady-state conditions, and each experimental point was averaged over at least three independent runs to ensure reproducibility. Data analysis focused on correlating plasma parameters such as electron density, optical emission intensity, and ion energy with the applied magnetic field strength and gas composition. This systematic approach enabled a comprehensive understanding of how magnetization influences microplasma behavior in next-generation semiconductor etching environments [28,29].

3. Results and Discussion

Figure (2) shows the variation of electron density with magnetic field strength in a magnetized microplasma. As the magnetic field increases from 0 to 200 G, the electron density rises rapidly and gradually saturates near higher fields. This behavior indicates improved electron confinement due to the Lorentz force, which reduces electron loss to the walls and enhances ionization efficiency.

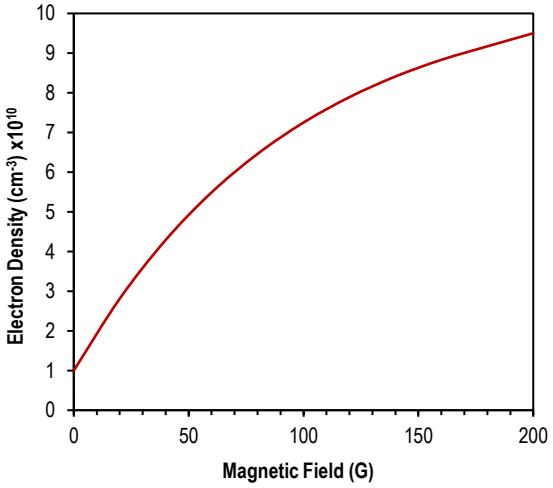

Fig. (2) Variation of electron density in CF_4/O_2 microplasmas with applied external magnetic field

The saturation region suggests that beyond a certain field strength, additional magnetization yields diminishing gains in plasma density, likely due to reduced electron mobility and increased collision frequency. Overall, the trend confirms that moderate magnetic confinement effectively enhances plasma density and stability [30].

Figure (3) illustrates the dependence of the silicon etching rate on magnetic field strength in a magnetized microplasma. The etch rate increases sharply as the magnetic field rises, reaching a maximum around 100–120 G, followed by a gradual decline at higher fields. The initial enhancement results from improved plasma confinement and increased ionization, leading to a higher flux of energetic ions toward the substrate. Beyond the optimal field, excessive confinement reduces ion energy and transport efficiency, lowering the etch rate. This trend indicates the existence of an optimum magnetic field range that maximizes anisotropic etching efficiency and process uniformity [31,32].

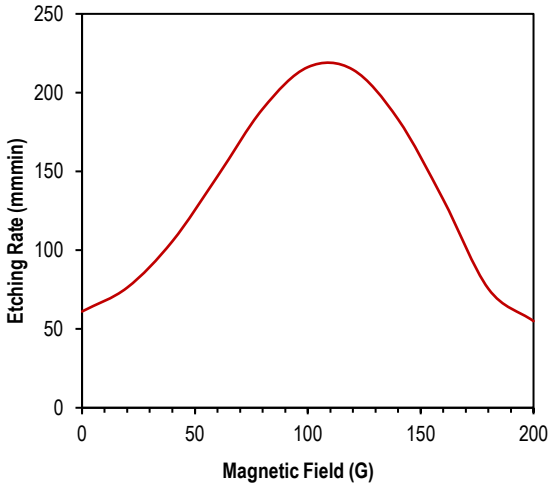

Fig. (3) Effect of magnetic field strength on the etching rate of silicon substrates exposed to magnetized CF_4/O_2 microplasmas

4. Conclusions

In conclusion, this study successfully demonstrated the development and characterization of a compact, low-pressure magnetized microplasma source optimized for next-generation semiconductor etching applications. Experimental results confirmed that the application of a controlled magnetic field significantly enhances plasma confinement, electron density, and overall process stability. The electron density increased with magnetic field strength, indicating improved ionization efficiency and reduced particle loss, while the etch rate exhibited an optimal range around 100–120 G, balancing ion flux and energy. These findings establish that magnetic confinement enables precise control of plasma properties, leading to improved etching anisotropy, uniformity, and reduced substrate damage. Consequently, the proposed magnetized microplasma reactor offers a scalable and energy-efficient platform for sub-10 nm patterning and advanced microelectronics fabrication.

References

[1] G. Wypych, "5 - Microscopic Mechanisms of Damage Caused by Degradants", G. Wypych (ed.), Atlas of Material Damage, Elsevier (2012), pp. 105-283.

[2] A. Yamaguchi, A. Hirohata and B.J.H. Stadler (eds.), "Sensor and System", Ch. 8, in Micro and Nano Technologies, Nanomagnetic Materials, Elsevier (2021), pp. 579-622.

[3] G.A. Marcelo et al., "Magnetic, fluorescent and hybrid nanoparticles: From synthesis to application in Biosystems", Mater. Sci. Eng. C, 106 (2020) 110104.

[4] B.T. Chiad et al., "Characteristics and operation conditions of a closed-field unbalanced dual magnetrons plasma sputtering system", Open Access Lib., 1(6) (2014) 1-7.

[5] J. Koskinen, "Cathodic-Arc and Thermal-Evaporation Deposition", S. Hashmi, G.F. Batalha, C.J. Van Tyne, Bekir Yilbas (eds.), Comprehensive Materials Processing, Elsevier (2014), pp. 3-55.

[6] M. Keidar and I.I. Beilis, "Chapter 6 - Plasma Nanoscience and Nanotechnology", M. Keidar, I.I. Beilis (eds.), Plasma Engineering, Academic Press (2013), pp. 287-357.

[7] B.D. Guenther and D.G. Steel (eds.), Encyclopedia of Modern Optics, 2nd ed., Elsevier (2017), pp. 331-394.

[8] C. Li et al., "Progress in reactions, momentum transfer, and energy transfer processes for nanoparticles in processing non-thermal plasmas, *Phys. Rep.*, 1135 (2025) 1-73.

[9] M. Keidar and I.I. Beilis, Chapter 6 - Plasma Nanoscience and Nanotechnology, M. Keidar and I.I. Beilis (eds.), Plasma Engineering, 2nd ed., Academic Press (2018), pp. 365-453.

[10] G. Wypych (ed.), Atlas of Material Damage, 2nd ed., ChemTec Publishing (2017), pp. 307-333.

[11] M. Uenohara, Cooled Varactor Parametric Amplifiers, L. Young (ed.), Advances in Microwaves, vol. 2, Elsevier (1967), pp. 89-164.

[12] A. Dubey and C.L. Dube, "Microwave processing of carbon-based materials: A review", *Nano-Struct. Nano-Objects*, 38 (2024) 101136.

[13] Z.H. Zaidan, O.A. Hammadi and K.H. Mahmood, "Effect of Structural Phase on Photocatalytic Activity of Titanium Dioxide Nanoparticles", Iraqi J. Appl. Phys., 19(3A) (2023) 55-58.

[14] D. Tan et al., "Femtosecond laser induced phenomena in transparent solid materials: Fundamentals and applications", *Prog. Mater. Sci.*, 76 (2016) 154-228.

[15] P. Worsfold, C. Poole, A. Townshend and M. Miró (eds.), Encyclopedia of Analytical Science, 3rd ed., Academic Press (2019), pp. 483-548.

[16] C. Marton (ed.), Advances in Electronics and Electron Physics, vol. 56, Academic Press (1981), pp. 291-358.

[17] G. Wypych (ed.), Atlas of Material Damage, Elsevier (2012), pp. 285-311.

[18] J.-P. Deville and C.S. Cojocaru, Chapter 12 - Spectroscopic Analyses of Surfaces and Thin Films,

Y. Pauleau (ed.), in European Materials Research Society Series, Materials Surface Processing by Directed Energy Techniques, Elsevier (2006), pp. 411-441.

[19] M.K. Khalaf, O.A. Hammadi and F.J. Kadhim, "Current-voltage characteristics of dc plasma discharges employed in sputtering techniques", Iraqi J. Appl. Phys., 12(3) (2016) 11-16.

[20] Y. Setsuhara, Plasma Sources in Thin Film Deposition, S. Hashmi, G.F. Batalha, C.J. Van Tyne, B. Yilbas (eds.), Comprehensive Materials Processing, Elsevier (2014), pp. 307-324.

[21] K. Wandelt (ed.), Encyclopedia of Interfacial Chemistry, Elsevier (2018), pp. 551-629.

[22] H.H. Wieder, Devices and Applications, Ch. 5, H.H. Wieder (ed.), in International Series of Monographs in Semiconductors, Intermetallic Semiconducting Films, Pergamon (1970), pp. 231-288.

[23] G.R. Jones, M.A. Laughton and M.G. Say (eds.), Electrical Engineer's Reference Book, 5th ed., Newnes (1993), pp. 1-27.

[24] A. Martucci, L. Santos, R.E. Rojas Hernández, R. Almeida (eds.), in Woodhead Publishing Series in Electronic and Optical Materials, Sol-Gel Derived Optical and Photonic Materials, Woodhead Publishing (2020), pp. 369-382.

[25] P.W. Hawkes (ed.), Advances in Imaging and Electron Physics, vol. 104, Elsevier (1998), pp. 1-380.

[26] P. Pai and M. Tabib-Azar, "Micro-Plasma Field Effect Transistor Operating with DC Plasma", IEEE Electron Dev. Lett., 35 (2014) 593–595.

[27] V.J. Vipu Vinayak et al., "Conducting polymer based nanocomposites for supercapacitor applications: A review of recent advances, challenges and future prospects", *J. Ener. Stor.*, 100(B) (2024) 113551.

[28] G. Wypych, 5 - Microscopic Mechanisms of Damage Caused by Degradants, G. Wypych (ed.), Atlas of Material Damage, 2nd ed., ChemTec Publishing (2017), pp. 113-305.

[29] K. Searles et al., "A planar micro rotary actuator for endoscopic optical scanning", *Sens. Actuat. A: Phys.*, 345 (2022) 113768.

[30] G. Wypych, 5 - Microscopic Mechanisms of Damage Caused by Degradants, G. Wypych (ed.), Atlas of Material Damage, 3rd ed., ChemTec Publishing (2022), pp. 141-386.

[31] M.A. Laughton and D.J. Warne (eds.), Electrical Engineer's Reference Book, 16th ed., Newnes (2003), pp. 1-22.

[32] R.K. Willardson and E.R. Weber (eds.), Semiconductors and Semimetals, vol. 53, Elsevier (1998), pp. 1-390.

